



引文格式: 孙崇波, 周洪兵, 谢万洪, 等. 哀牢山构造带南段早泥盆世硅质岩形成环境及大地构造意义[J]. 西北地质, 2025, 58(5): 140–150. DOI: 10.12401/j.nwg.2024127

Citation: SUN Chongbo, ZHOU Hongbing, XIE Wanhong, et al. Depositional Environments and Tectonic Background of the Early Devonian Cherts of Southern Ailaoshan Tectonic Belt[J]. Northwestern Geology, 2025, 58(5): 140–150. DOI: 10.12401/j.nwg.2024127

哀牢山构造带南段早泥盆世硅质岩形成 环境及大地构造意义

孙崇波^{1,2}, 周洪兵^{1,2}, 谢万洪¹, 李敏同^{1,2}, 杨洪伟^{1,*}

(1. 四川省金属地质调查研究所, 四川 成都 611730; 2. 周洪兵青年创新工作室, 四川 成都 611730)

摘要:金沙江-哀牢山构造带在晚古生代发育的是古特提斯支洋还是弧后盆地尚存在争论,笔者对哀牢山构造带南段下泥盆统硅质岩开展岩相学、岩石地球化学等分析,以期为该地区构造演化提供新的证据。硅质岩地球化学特征显示出其为生物成因, SiO_2 与 Al_2O_3 、 SiO_2 与 TiO_2 具明显负相关性,说明硅质不是来自陆源物质,具 Ce 负异常, Ce/Ce^* 值为 $0.73 \sim 0.76$, 平均值为 0.75 , 接近大洋盆地硅质岩特征; $(\text{La}/\text{Ce})_N$ 值为 $1.31 \sim 1.49$, 平均为 1.38 , 接近开阔洋盆硅质岩特征。综合分析认为,硅质岩形成于边缘海向开阔大洋转换的环境,暗示金沙江-哀牢山构造带在晚古生代发育的是古特提斯支洋,而非弧后盆地。

关键词: 哀牢山构造带南段; 放射虫硅质岩; 形成环境; 哀牢山支洋

中图分类号: P581; P548

文献标志码: A

文章编号: 1009-6248(2025)05-0140-11

Depositional Environments and Tectonic Background of the Early Devonian Cherts of Southern Ailaoshan Tectonic Belt

SUN Chongbo^{1,2}, ZHOU Hongbing^{1,2}, XIE Wanhong¹, LI Mintong^{1,2}, YANG Hongwei^{1,*}

(1. Sichuan Institute of Metal Geology, Chengdu 611730, Sichuan, China; 2. ZHOU Hongbing Youth Innovation Studio, Chengdu 611730, Sichuan, China)

Abstract: There is still a debate about whether the Jinshajiang Ailaoshan tectonic belt developed in the Late Paleozoic was a Paleo Tethyan Ocean or a backarc basin. This paper conducts petrographic and geochemical analyses of the Lower Devonian siliceous rocks in the southern section of the Ailaoshan tectonic belt in order to provide new evidence for the tectonic evolution of the area. The geochemical characteristics of siliceous rocks show that they are biogenic, with a significant negative correlation between SiO_2 and Al_2O_3 , and SiO_2 and TiO_2 , indicating that siliceous rocks do not come from terrestrial sources and have a negative Ce anomaly. The Ce/Ce^* value is 0.73 to 0.76, with an average value of 0.75, which is close to the characteristics of siliceous rocks in

收稿日期: 2024-12-22; 修回日期: 2024-12-25; 责任编辑: 曹佰迪

基金项目: 中国地质调查局项目“西南三江成矿带南段基础地质调查”(1212010880406、1212011120582)资助。

作者简介: 孙崇波(1985-), 男, 高级工程师, 博士, 主要从事地质调查与矿产勘查研究。E-mail: 1315333036@qq.com。

* 通讯作者: 杨洪伟(1980-), 男, 高级工程师, 地质调查与矿产勘查。E-mail: 37552816@qq.com。

ocean basins; The La_N/Ce_N value ranges from 1.31 to 1.49, with an average of 1.38, which is close to the characteristics of siliceous rocks in open ocean basins. Based on comprehensive analysis, it is believed that the siliceous rocks were formed in a transitional environment from marginal seas to open oceans, suggesting that the Jinshajiang Ailaoshan tectonic belt developed in the Late Paleozoic in the Paleo Tethyan Ocean rather than in a backarc basin.

Keywords: southern Ailaoshan tectonic belt; radiolarian bedded chert; depositional environments; Ailaoshan branch

硅质岩作为一种特殊的沉积岩,其成因主要为热水沉积成因、正常海水沉积成因、生物成因(含有放射虫、海绵骨针、蓝藻等),物质来源主要为陆源碎屑、生物新陈代谢物质及遗体、热水萃取海底地层、火山物质等,其矿物组成和演化序列一般为蛋白石-A(opal-A)→蛋白石-CT(opal-CT)→玉髓→石英(Miroshnichenko et al., 2010; Yin et al., 2016; Lewis et al., 2016)。因为硅质岩的岩石学、地球化学、矿物学性质稳定,其原始沉积环境等信息可以得到较好的保存(Murry et al., 1990, 1991, 1994),所以硅质岩常被用于研究古环境变化和构造演化(Chakrabarti et al., 2012; Thurston et al., 2012; Fan et al., 2013),对古特提斯洋的演化存在很好的指示作用(Hara et al., 2010; Thassanapak et al., 2011; Huang et al., 2013)。

哀牢山造山带位于特提斯-喜马拉雅构造区与滨太平洋构造区的接触部位(图1),兼具印支思茅地块和扬子地块两大构造单元的属性(钟大赉, 1998; 方维萱等, 2002; Fan et al., 2010; 孙崇波等 2016),众多学者

通过地球化学、年代学、地球动力学等方面对其进行研究(Molnar et al., 1975; Schärer et al., 1990; Tapponnier et al., 1990; 钟大赉, 1998; Metcalfe, 2006; 刘翠等, 2011; Xia et al., 2016; 孙崇波等, 2016, 2017, 2018, 2019)。然而,金沙江-哀牢山构造带在晚古生代发育的是古特提斯支洋还是弧后盆地尚存在争论,目前主要有两种观点:一种观点认为在金沙江-哀牢山-松马构造带发育了支洋盆(Jian et al., 2009a, 2009b; Wang et al., 2014; 孙崇波等 2016);而另一种则认为发育了古特提斯洋东缘弧后盆地(Metcalfe, 2006; Fan et al., 2010; 2013)。而且,关于其打开机制与时限同样存在争议:部分学者认为金沙江-哀牢山洋形成自石炭纪一二叠纪昌宁—孟连主洋盆的弧后洋盆(Metcalfe, 2006, 2013; Fan et al., 2010; Pan et al., 2012);部分学者认为洋盆打开于泥盆纪,并经历了完整的威尔逊旋回(魏启荣等, 1998; 方维萱等, 2002; 刘兵兵等, 2017)。

笔者借鉴前人对硅质岩的研究成果,对哀牢山构造带南段早泥盆世(保红组)硅质岩进行了主量元素

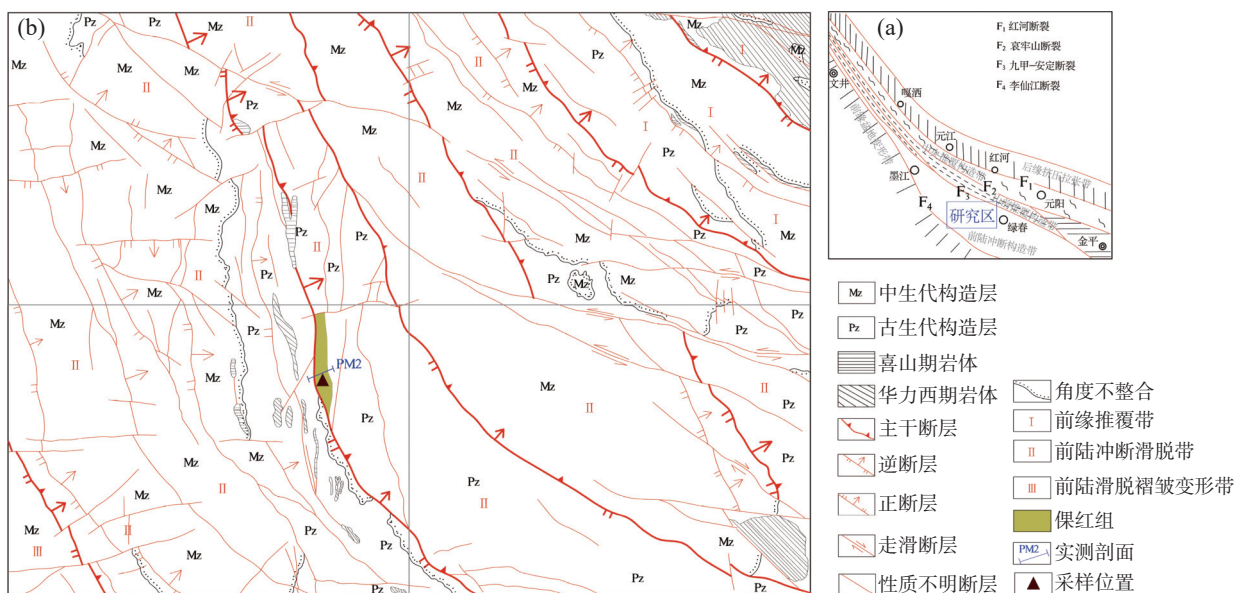


图1 哀牢山构造带南段构造图(a)及研究区地质略图(b)

Fig. 1 (a) Structural map of the southern Ailaoshan tectonic belt, and (b) geological sketch map of the study area

及稀土元素分析,进一步研究其成因类型、形成环境,以期对该地区的构造演化提供新的证据。

1 地质背景及样品特征

笔者采集的硅质岩样品位于哀牢山构造带南段,哀牢山断裂西侧,绿春县北部,下泥盆统保红组PM2实测地质剖面中。剖面上保红组未见底,与晚二叠世羊八寨组呈断层接触,其上依次为大中寨组、龙别组,保红组与大中寨组呈整合接触,大中寨组与龙别组呈断层接触,上未见顶,与石炭系上段呈断层接触。硅质岩为灰色,呈层状与泥岩互层,中间夹中-厚层状灰岩(图2)。在光学显微镜下可见粒序层理及水平层理构造,显示出沉积硅质岩的特征,且硅质岩中均见有放射虫化石(图3)。本次样品采集发现地层岩石中含大量化石(图4),其中有笔石 *Neomonograptus hercynicus*, *Monograptus cf. hermiodon*, 竹节石 *Paranowakia* sp.等化石,属下泥盆统洛霍考夫阶(Lochkonian); *Monograptus yukounensis fangensis*, 竹节石 *Ten-*

taacultes sp., *Nowakia acuaria*(尖锐塔节石)等,属下泥盆统布拉格阶(Pragian);竹节石 *Nowakia zilchovensis* 等,属下泥盆统埃姆斯阶(Emsian)。经南京地质古生物研究所鉴定,所含竹节石皆为 *Nowakia* sp., *Styliodima* sp., *Striatostylioma* sp., 属下泥盆统。*Polygnathus dehiscens-Pandorinellina steinhornensis* 牙形石,其中 *Polygnathus dehiscens* 是下泥盆统埃姆斯阶底带的化石, *Pandorinellina steinhornensis* 在国内外一般见于下泥盆统埃姆斯阶, *Ozarkodina kurtosa* 的时限为埃姆斯期, *Ozarkodina denckmanni* 多见于埃姆斯期,为早泥盆世的牙形石。

2 采样及测试方法

笔者采集的样品共计6件,岩性均为放射虫硅质岩。样品主量元素及稀土元素分析测试均在四川省冶金地质岩矿测试中心完成。常量元素:在制备好的粉样中添加 $\text{Li}_2\text{B}_4\text{O}_7$ - LiBO_2 助熔物质,进行充分混合,于1000 °C 熔融。待熔融物质冷却后加入稀硝酸和稀

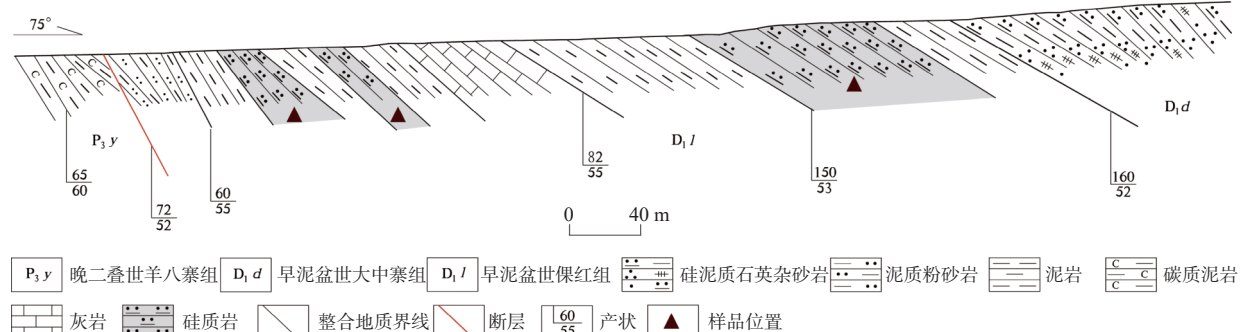


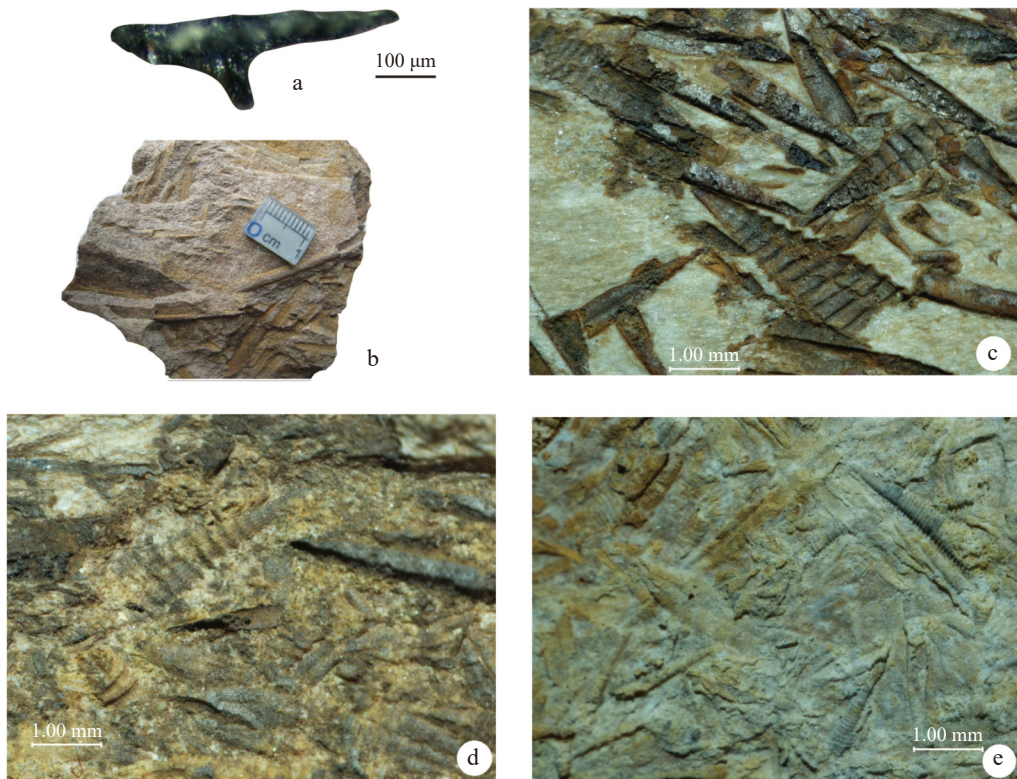
图2 下泥盆统保红组PM2实测剖面

Fig. 2 PM2 Measured section of Lower Devonian Luohong Formation



图3 下泥盆统保红组放射虫硅质岩

Fig. 3 Radiolarian silicalite of Lower Devonian Luohong Formation



a.*Polygnathus dehiscens*; b.竹节石; c.*Neomonograptus hercynicus*; d.*Monograptus cf. hermiodon*; e.*Paranowakia* sp

图4 下泥盆统保红组化石

Fig. 4 Early Devonian fossils of Lower Devonian Luohong Formation

盐酸溶解,用电感耦合等离子体发射光谱仪利用ME-ICP06方法定量测试。各元素分析精度(RSD): SiO_2 为0.8%, Al_2O_3 为0.5%, Fe_2O_3 为0.4%, MgO 为0.7%, TiO_2 为0.9%, P_2O_5 为0.8%, CaO 为0.6%, Na_2O 为0.3%, K_2O 为0.4%, MnO 为0.7%。将制备好的定量样品放入马弗炉中,进行1000 °C加热1 h,待冷却称重,计算样品加热前后的重量差,即为烧失量百分比。稀土元素分析: HF+HNO₃密封溶解,加入RH内标溶液,用1%硝酸定容,选用ME-MS81方法,通过电感耦合等离子质谱仪进行定量测试,分析精度优于5%。页岩稀土元素标准化值源自 Taylor 等(1985), $\text{Ce}/\text{Ce}^*=2\text{Ce}_N/(\text{La}_N+\text{Pr}_N)$, $\text{Eu}/\text{Eu}^*=2\text{Eu}_N/(\text{Sm}_N+\text{Gd}_N)$ (N为NASC标准化数值)。

3 硅质岩地球化学特征

3.1 主量元素特征

通过对早泥盆世保红组放射虫硅质岩主量元素分析(表1), 硅质岩 SiO_2 含量为 92.6%~95.9%, Al_2O_3 含量为 1.58%~3.12%, TiO_2 含量为 0.04%~0.11%,

表1 下泥盆统罗红组硅质岩主量元素(%)分析数据

Tab. 1 Major (%) compositions of Silicous rock from Lower Devonian Luohong Formation

样号	D ₁ -b1	D ₁ -b2	D ₁ -b3	D ₁ -b4	D ₁ -b5	D ₁ -b6
SiO_2	92.6	95.8	95.9	95.7	95.6	95.8
Al_2O_3	3.12	1.58	1.68	1.62	1.66	1.6
Fe_2O_3	1.88	1.14	1.04	1.17	1.22	1.35
FeO	0.13	0.19	0.14	0.31	0.89	0.30
P_2O_5	0.09	0.16	0.02	0.07	0.11	0.03
K_2O	0.71	0.35	0.38	0.36	0.35	0.37
Na_2O	0.07	0.04	0.02	0.03	0.02	0.03
MgO	0.12	0.07	0.07	0.08	0.06	0.06
CaO	0.04	0.02	<0.01	0.02	0.01	0.02
TiO_2	0.11	0.05	0.05	0.06	0.04	0.05
MnO	—	—	—	—	0.01	—
LoI	0.21	1.14	0.28	0.41	1.02	0.44
总量	98.95	100.35	99.44	99.52	100.1	99.75

Fe_2O_3 含量为 1.04%~1.88%。在 Al-Fe-Mn 图解中, 硅质岩样品均落在“非热液成因”区内(图 5), 说明其为生物化学成因。正常海相硅质岩的 Al、Ti、Fe 和 REE 含量较为稳定(Murray et al., 1992; Murray, 1994), 因而通常将 $\text{Fe}_2\text{O}_3/\text{TiO}_2$ - $\text{Al}_2\text{O}_3/(\text{Al}_2\text{O}_3+\text{Fe}_2\text{O}_3)$ 图解用来判别硅质岩成因和形成环境。在 $\text{Fe}_2\text{O}_3/\text{TiO}_2$ - $\text{Al}_2\text{O}_3/(\text{Al}_2\text{O}_3+\text{Fe}_2\text{O}_3)$ 图解中, 样品均落于大陆边缘及深海沉积的重叠区域(图 6), 说明其可能形成与受陆源物质影响的深海环境。通常情况下, 硅质岩中 Al_2O_3 及 TiO_2 含量随着陆源物质含量的增多而变大, 是硅质岩源区碎屑物质来源的判别标志(Murray, 1994)。笔者进一步分析了 6 件硅质岩中 SiO_2 与 Al_2O_3 、 SiO_2 与 TiO_2 及 Al_2O_3 与 TiO_2 的相互关系(图 7)。结果显示, TiO_2 及 Al_2O_3 具有明显的关系, 硅质岩中 SiO_2 与 Al_2O_3 、 SiO_2 与 TiO_2 不具正相关性, 但具明显的负相关性, 呈现此消彼长的趋势, 说明陆源物质不是硅质来源, 硅质可能来源于生物有机质自海水中摄取。

3.2 稀土元素特征

海水中 $\sum\text{REE}$ 的主要物质来源是地表河流, 大陆架中海水的稀土元素地球化学特征受地表河流的影响巨大(Chen et al., 2006)。硅质岩作为一种特殊的积岩, 其表现出非常强的继承性, 当其未遭受陆源物质混入或者未受到热液活动影响时, 其 $\sum\text{REE}$ 的物质来源主要为海水(Murray et al., 1991), 但当其受到路远物质混入或者收到热液活动影响后, 则其 $\sum\text{REE}$ 会发生明显的改变(Murray, 1994; Qiu et al., 2011a, 2011b; Huang et al., 2012)。因此, 可通过稀土元素组成研究, 来判断硅质岩及其共生矿床的成因和构造环境的识别(Chen et al., 2006; Fan et al., 2013; Huang et al., 2013)。

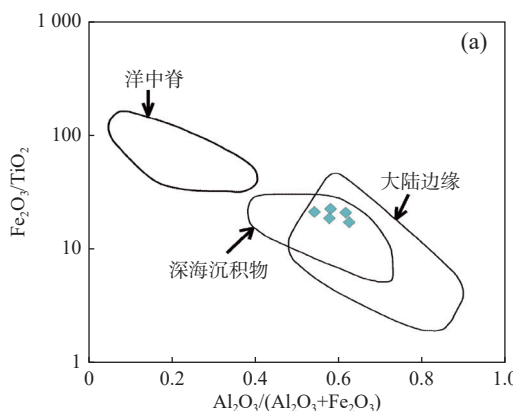


图 6 $\text{Fe}_2\text{O}_3/\text{TiO}_2$ - $\text{Al}_2\text{O}_3/(\text{Al}_2\text{O}_3+\text{Fe}_2\text{O}_3)$ (a) 及 La_N/Ce_N - $\text{Al}_2\text{O}_3/(\text{Al}_2\text{O}_3+\text{Fe}_2\text{O}_3)$ (b) 图解(据 Murray, 1994)

Fig. 6 (a) $\text{Fe}_2\text{O}_3/\text{TiO}_2$ - $\text{Al}_2\text{O}_3/(\text{Al}_2\text{O}_3+\text{Fe}_2\text{O}_3)$ and (b) La_N/Ce_N - $\text{Al}_2\text{O}_3/(\text{Al}_2\text{O}_3+\text{Fe}_2\text{O}_3)$ diagram

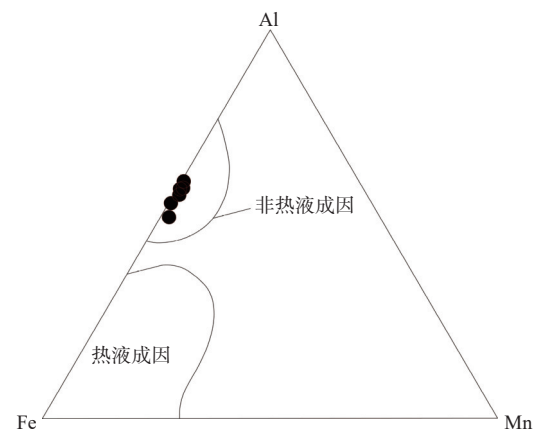


图 5 下泥盆统罗红组硅质岩类 Al-Fe-Mn 判别图解图
(据 Adachi M et al., 1986)

Fig. 5 Al-Fe-Mn diagram Fig of Lower Devonian Luohong Formation silicilite

早泥盆世罗红组放射虫硅质岩沉积物稀土元素分析结果及参数特征见表 2, 稀土元素北美页岩标准化模式图见图 8。稀土元素北美页岩标准化模式图显示, 所有样品曲线表现为平坦型, 轻、重稀土元素分异相对不明显, 具 Ce 负异常特征。硅质沉积物 $\sum\text{REE}$ 含量为 $21.29 \times 10^{-6} \sim 37.66 \times 10^{-6}$, 平均为 27.34×10^{-6} , 数值相对偏低。

硅质岩 Ce/Ce* 值作为表征成岩环境的重要参数被广泛使用(Murray et al., 1991, 1992; Hara et al., 2010; 黄虎等, 2012; Huang et al., 2013)。在深海环境下, 由于受到陆源物质影响小, 海水中的 Ce 往往以 Ce^{4+} 的形态渗透至锰结核内, 其 Ce 显示出正异常(Fleet, 1983; Bau et al., 1996), 或者海水中的 Ce 与氧结合, 从而形成难溶解的铈氧化物, 导致海水显示出 Ce 负异常(Elderfield et al., 1982); 当存在大量陆源物质参与其中,

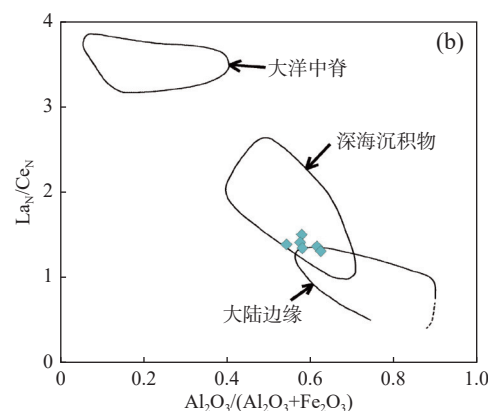
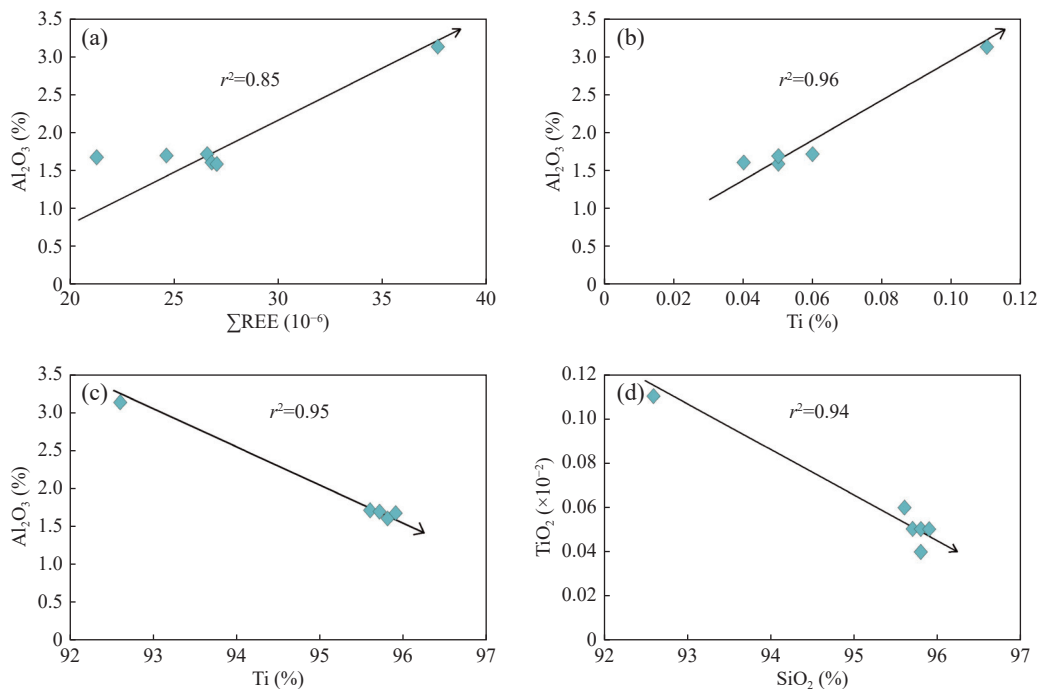


图 6 $\text{Fe}_2\text{O}_3/\text{TiO}_2$ - $\text{Al}_2\text{O}_3/(\text{Al}_2\text{O}_3+\text{Fe}_2\text{O}_3)$ (a) 及 La_N/Ce_N - $\text{Al}_2\text{O}_3/(\text{Al}_2\text{O}_3+\text{Fe}_2\text{O}_3)$ (b) 图解(据 Murray, 1994)

Fig. 6 (a) $\text{Fe}_2\text{O}_3/\text{TiO}_2$ - $\text{Al}_2\text{O}_3/(\text{Al}_2\text{O}_3+\text{Fe}_2\text{O}_3)$ and (b) La_N/Ce_N - $\text{Al}_2\text{O}_3/(\text{Al}_2\text{O}_3+\text{Fe}_2\text{O}_3)$ diagram

图7 下泥盆统罗红组硅质沉积物 Al_2O_3 、 SiO_2 与其他元素相关性图解Fig. 7 Geochemical correlation diagrams between Al_2O_3 , SiO_2 with other elements from Lower Devonian Luohong Formation表2 下泥盆统罗红组硅质岩稀土元素丰度(10^{-6})及主要参数Tab. 2 REE analyses of Silicous rock Lower Devonian Luohong Formation (10^{-6})

样号	D ₁ -b1	D ₁ -b2	D ₁ -b3	D ₁ -b4	D ₁ -b5	D ₁ -b6
La	7.9	6.9	4.5	5.6	6.2	6.4
Ce	12.9	9.9	7.1	8.9	9.4	9.1
Pr	1.81	1.26	1.02	1.11	1.2	1.18
Nd	7.0	4.5	3.9	4.1	4.4	4.5
Sm	1.48	0.88	0.9	0.93	1.12	1.21
Eu	0.35	0.21	0.22	0.23	0.25	0.23
Gd	1.72	1.02	0.97	0.99	1.12	1.24
Tb	0.31	0.18	0.21	0.2	0.19	0.21
Dy	1.57	0.81	1.02	1.1	1.06	0.97
Ho	0.37	0.17	0.22	0.19	0.18	0.22
Er	1.02	0.51	0.58	0.5	0.54	0.65
Tm	0.15	0.08	0.08	0.09	0.11	0.1
Yb	0.94	0.54	0.5	0.61	0.72	0.71
Lu	0.14	0.08	0.07	0.08	0.09	0.1
ΣREE	37.66	27.04	21.29	24.63	26.58	26.82
LREE/HREE	5.05	6.98	4.83	5.55	5.63	5.39
La_N/Yb_N	0.79	1.20	0.85	0.87	0.81	0.85
Ce/Ce^*	0.76	0.73	0.74	0.75	0.76	0.75
(La/Ce) _N	1.31	1.49	1.36	1.34	1.41	1.38

硅质岩 Ce/Ce^* 值显现出正异常。Murray 等(1990, 1991)在研究了加利福尼亚佛朗西斯科岩群中的硅质岩后, 得出自大洋中脊附近→大洋盆地→大陆边缘, 其 Ce/Ce^* 值分别为 0.17~0.56(平均 0.28)→0.47~0.71(平均 0.60)→0.62~1.43(平均 1.03)。笔者研究的硅质岩 Ce/Ce^* 值为 0.73~0.76, 平均值为 0.75, 值更接近于“大洋盆地”硅质岩。

Girty 等(1996)研究认为, 通常与大陆边缘弧相关的沉积物 $(\text{La}/\text{Ce})_N$ 值 < 1, 大洋深海沉积物 $(\text{La}/\text{Ce})_N$ 值为 2.0~3.0, 靠近洋中脊沉积物 $(\text{La}/\text{Ce})_N$ 值 > 3.5。Murray 等(1991)研究认为, 形成于开阔洋盆硅质岩的 $(\text{La}/\text{Ce})_N$ 值为 1.30~2.48, 平均为 1.81。Qiu 等(2011a)研究认为, 形成于受陆源物质影响的边缘海盆硅质岩 $(\text{La}/\text{Ce})_N$ 值为 1.46~3.37, 平均为 2.07。杨振宇等(2009)研究认为, 形成于大洋中脊附近硅质岩的 $(\text{La}/\text{Ce})_N$ 值 > 3.5, 与 Girty 等(1996)的观点一致。笔者研究的硅质岩 $(\text{La}/\text{Ce})_N$ 值为 1.31~1.49, 平均为 1.38, 更接近于开阔洋盆硅质岩特征。Murray(1994)通过研究得出, 硅质岩中 La 与 Ce 北美页岩标准化比值 $(\text{La}/\text{Ce})_N$ 与 $\text{Al}_2\text{O}_3/(\text{Al}_2\text{O}_3+\text{Fe}_2\text{O}_3)$ 未受到成岩作用过程的影响, 说明 $(\text{La}/\text{Ce})_N$ 与 $\text{Al}_2\text{O}_3/(\text{Al}_2\text{O}_3+\text{Fe}_2\text{O}_3)$ 值能够客观的反映出硅质岩的形成环境。笔者研究的硅质岩在 $(\text{La}/\text{Ce})_N-\text{Al}_2\text{O}_3/(\text{Al}_2\text{O}_3+\text{Fe}_2\text{O}_3)$ 图解中, 6 件样品

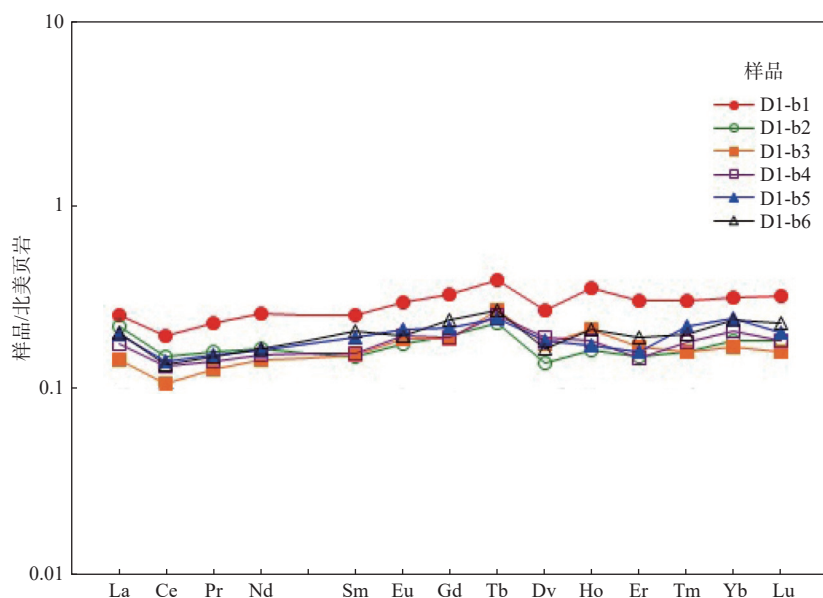


图8 下泥盆统罗红组硅质岩北美页岩标准化模式图(据 Taylor et al., 1985)

Fig. 8 Shale-normalized REE distribution patterns of Siliceous from Lower Devonian Luohong Formation

均落于深海沉积物区(图6)，其中3件样品落于深海沉积物与大陆边缘沉积物重叠区域，说明硅质岩沉积环境逐渐远离大陆边缘，主要为深海沉积，这与主量元素显示的沉积物中硅质不是来自陆源物质的结论相符。

4 大地构造意义

魏启荣等(1998)对哀牢山硅质岩特征的研究认为，哀牢山晚泥盆世(D_3)硅质岩形成于深海环境，说明扬子地台西缘在该时期已裂开了一个深海槽；早石炭世(C_1)硅质岩形成于半深海环境，该时期扬子地台西缘已拉张形成了洋壳，为规模不大的洋盆。

此外，哀牢山断裂带东侧(扬子地块西缘)下泥盆统岩性主要为灰白、灰黄色石英砂岩，笔者研究区位于哀牢山断裂带西部，下泥盆统岩性自下至上依次为粉砂岩、泥岩互层-泥岩、硅质岩互层-中厚层灰岩-泥岩-泥岩硅质岩互层(图9)。哀牢山断裂带两侧下泥盆统岩性存在很大差异，说明其物源不同，暗示哀牢山断裂带存在一个深水盆地，导致两侧物源差异，从而沉积了不同的岩石组合。

Jian等(2009b)在金沙江蛇绿岩套中发现了原岩为大陆溢流相玄武岩的闪长岩包体，其年龄为439~404 Ma，测得辉绿岩锆石U-Pb年龄为 (382.9 ± 3.9) Ma，在双沟蛇绿岩带内测得斜长花岗岩U-Pb年龄为

(375.9 ± 4.2) Ma。Chun等(2014)在双沟蛇绿岩带内获得斜长花岗岩锆石U-Pb年龄为 (405 ± 6.6) Ma的继承锆石。简平等(1998)测得龙塘辉长岩的锆石U-Pb下交点年龄为 (362 ± 41) Ma。以上结论均说明作为整体的印支—扬子陆块至少在晚志留世已经发生大陆裂解，形成了大陆裂谷，并在中泥盆世之前就已经开始了大规模海底扩张。刘兵兵等(2017)通过对碎屑锆石年代学研究，发现早泥盆世哀牢山断裂带两侧物源存在明显差异，认为在早泥盆世晚期哀牢山造山带已经形成了开阔的大洋，与文中观点一致。

刘汇川等(2014)通过对哀牢山蛇绿岩微量元素的总结研究，得出哀牢山蛇绿岩地球化学特征不具E-MORB，更不是弧后盆地蛇绿岩地球化学特征，而与N-MORB一致。此外，众多学者对双沟地区蛇绿岩研究表明，其更接近印度洋MORB特征，指示蛇绿岩来自具DUPAL异常的地幔源区(Jones et al., 1984; 魏启荣等, 1995; 钟大赉, 1998; Xu et al., 2004)。也说明哀牢山构造带在晚古生代发育的是古特提斯支洋盆而非弧后盆地。

笔者研究的早泥盆世放射虫硅质岩为非热水沉积成因，形成于边缘海盆向开阔大洋转换的深水环境。说明在早泥盆世之前印支与扬子板块已经发生大陆裂解，于早泥盆世已演化为边缘海向开阔大洋的转换，哀牢山支洋盆(弧后盆地)在早泥盆世持续海底扩张，并初具开阔大洋的特征，表明哀牢山构

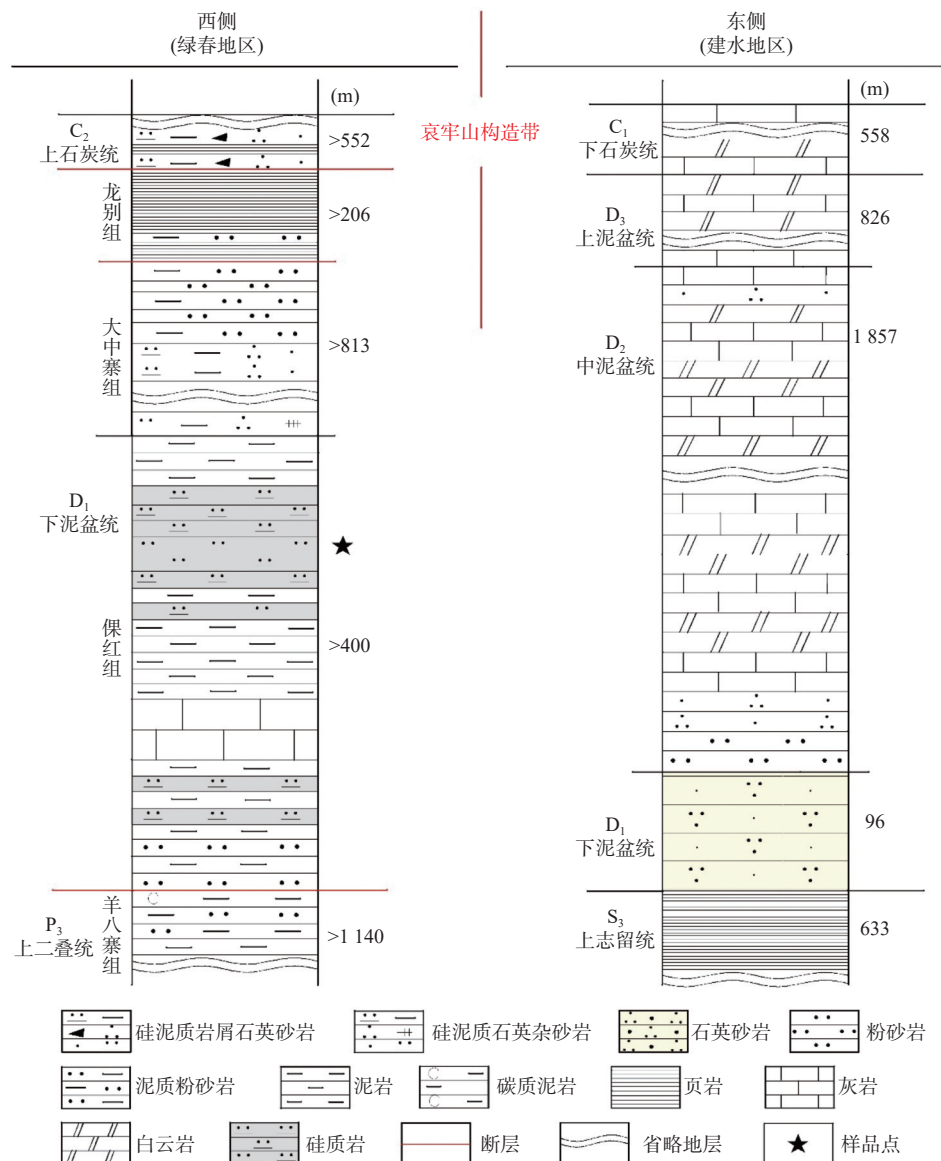


图9 哀牢山断裂两侧下泥盆统地层柱状图(东侧地层据云南省地质矿产局, 1990; 西侧为实测)

Fig. 9 Stratigraphic columns of lower Devonian strata both sides of the Ailaoshan Fault

造带在晚古生代发育的是古特提斯支洋盆,而不是弧后盆地。

5 结论

(1) 哀牢山构造带南段西边早泥盆世硅质岩属于生物成因, 硅质来源不是陆源物质, 其形成于边缘海盆向开阔大洋转换的深水环境。

(2) 通过硅质岩的形成环境可知哀牢山构造带在晚古生代发育的是哀牢山支洋, 并非弧后盆地。

(3) 作为整体的印支-扬子地块大陆裂解发生于

在泥盆世以前, 在早泥盆世时哀牢山支洋盆已初具开阔大洋形态。

参考文献(References):

- 方维萱, 胡瑞忠, 谢桂青, 等. 云南哀牢山地区构造岩石地层单元及其构造演化[J]. 大地构造与成矿学, 2002, 26(1): 28-36.
FANG Weixuan, HU Ruizhong, XIE Guiqing, et al. Tectono-lithostratigraphic units of the ailaoshan area in Yunnan, China and their implications of tectonic evolution[J]. Geotecttonica et Metallogenica, 2002, 26(1): 28-36.

- 黄虎, 杜元生, 杨江海, 等. 水城-紫云-南丹裂陷盆地晚古生代硅质沉积物地球化学特征及其地质意义 [J]. 地质学报, 2012, 86(12): 1994–2010.
- HUANG Hu, DU Yuansheng, YANG Jianhai, et al. Geochemical features of siliceous sediments of the Shuicheng-Ziyun-Nandan rift basin in the Late Paleozoic and their tectonic implication [J]. *Acta Geologica Sinica*, 2012, 86(12): 1994–2010.
- 简平, 汪啸风, 何龙清, 等. 云南新平县双沟蛇绿岩 U-Pb 年代学初步研究 [J]. 岩石学报, 1998, 14(2): 207–211.
- JIAN Ping, WANG Xiaofeng, HE Longqing, et al. A preliminary study U-Pb geochronology of the Shuang Gou ophiolite in Xinpingle County, Yunnan [J]. *Acta Petrologica Sinica*, 1998, 14(2): 207–211.
- 刘兵兵, 碰头平, 范蔚茗, 等. 哀牢山构造带两侧上志留—下泥盆统碎屑锆年代学: 物源及其构造意义 [J]. 大地构造与成矿学, 2017, 3(14): 1–19.
- LIU Bingbing, PENG Touping, FAN Weiming, et al. Geochronology of Detrital Zircon from the Upper Silurian–Lower Devonian Sedimentary Rocks at both Sides of the Ailaoshan Tectonic Zone: Provenance and Geological Significance [J]. *Geotectonica et Metallogenica*, 2017, 3(14): 1–19.
- 刘翠, 邓晋福, 刘俊来, 等. 哀牢山构造岩浆带晚二叠世—早三叠世火山岩特征及其构造环境 [J]. 岩石学报, 2011, 27(12): 3599–3602.
- LIU Cui, DENG Jinfu, LIU Junlai, et al. Characteristics of volcanic rocks from Late Permian to Early Triassic in Ailaoshan tectono-magmatic belt and implications for tectonic settings [J]. *Acta Petrologica Sinica*, 2011, 27(12): 3599–3602.
- 刘江川. 云南哀牢山构造带晚古生代至早中生代岩浆岩成因及构造演化 [D]. 广州: 中国科学院广州地球化学研究所博士学位论文, 2014, 1–195.
- LIU Huichuan. Petrogenesis of Late Paleozoic to early Mesozoic magmatic rocks in the Ailaoshan area (SW Yunnan): implications for the evolution of the Paleo-Tethys [D]. Guangzhou: The degree of Doctor of Science of Guangzhou Institute of Geochemistry, Chinese Academy of Sciences, 2014, 1–195.
- 邱振, 王清晨, 严德天. 广西来宾蓬莱滩剖面中上二叠统硅质岩的地球化学特征及沉积背景 [J]. 岩石学报, 2011a, 27(10): 3141–3155.
- QIU Zhen, WANG Qingchen, YAN Detian. Geochemistry and sedimentary background of the Middle-Upper Permian cherts in the Penglaitan section, Laibin, Guangxi Province [J]. *Acta Petrologica Sinica*, 2011a, 27(10): 3141–3155.
- 邱振, 王清晨. 广西来宾中上二叠统硅质岩海底热液成因的地球化学证据 [J]. 中国科学: 地球科学, 2011b, 41(5): 725–737.
- QIU Zhen, WANG Qingchen. Geochemical evidence for submarine hydrothermal origin of the Middle-Upper Permian chert in Laibin of Guangxi, China [J]. *Science in China: Series D Earth Sciences*, 2010b, 41(5): 725–737.
- 孙崇波, 李忠权, 王道永. 哀牢山造山带南段扭只二长花岗斑岩地球化学特征及其锆石 U-Pb 年代学研究 [J]. 中国地质, 2016, 43(1): 111–119.
- SUN Chongbo, LI Zhongquan, WANG Daoyong, et al. Petrogeochemistry and zircon U-Pb chronology of the Niuzhi monzonitic porphyry in southern segment of Ailao Mountain tectonic belt [J]. *Geology in China*, 2016, 43(1): 111–119.
- 孙崇波, 李忠权, 王道永. 云南哀牢山构造带仰宗流纹斑岩锆石 U-Pb 年龄, 地球化学特征及构造意义 [J]. 地质通报, 2017, 36(2–3): 190–198.
- SUN Chongbo, LI Zhongquan, WANG Daoyong, et al. Petrogeochemistry and zircon U-Pb chronology of the Yangzong rhyolite porphyry of Ailaoshan tectonic belt [J]. *Geological Bulletin of China*, 2017, 36(2–3): 190–198.
- 孙崇波, 李忠权, 陈晓东. 哀牢山构造带南段风别山霏细斑岩地球化学特征及其锆石 U-Pb 年代学研究 [J]. 地质论评, 2018, 64(5): 1251–1262.
- SUN Chongbo, LI Zhongquan, CHEN Xiaodong, et al. Petrogeochemistry and zircon U-Pb chronology of the Fengbieshan felsophyre in southern section of Ailaoshan tectonic belt [J]. *Geological Review*, 2018, 64(5): 1251–1262.
- 孙崇波, 李忠权, 王道永. 哀牢山构造带南段马玉花岗闪长岩地球化学特征及其锆石 U-Pb 年龄 [J]. 地质通报, 2019, 38(2–3): 223–230.
- SUN Chongbo, LI Zhongquan, WANG Daoyong, et al. Petrogeochemistry and zircon U-Pb age of the Mayu granodiorite in the southern section of Ailaoshan tectonic belt [J]. *Geological Bulletin of China*, 2019, 38(2–3): 223–230.
- 魏启荣, 沈上越. 哀牢山北段老王寨—浪泥塘一带蛇绿岩的形成环境 [J]. 特提斯地质, 1995, 19: 57–70.
- WEI Qirong, SHEN Shangyue. Depositional Environments of ophiolite in the Laowangzhai-Langnitang area in the northern part of Ailaoshan [J]. *Tethyan Geology*, 1995, 19: 57–70.
- 魏启荣, 沈上越, 莫宣学. 哀牢山硅质岩特征及其意义 [J]. 地质科技情报, 1998, 17(2): 29–34.
- WEI Qirong, SHEN Shangyue, MO Xuanxue. Characteristics and Significance of silicic acid in Ailaoshan area [J]. *Geological Science and Technology Information*, 1998, 17(2): 29–34.
- 杨振宇, 沈渭洲, 郑连弟. 广西来宾蓬莱滩二叠纪瓜德鲁普统一乐平统界限剖面元素和同位素地球化学研究及地质意义 [J]. 地质学报, 2009, 83(1): 1–15.
- YANG Zhenyu, SHEN Weizhou, ZHENG Liandi. Element and isotopic geochemistry of Guadalupian-Lopingian boundary profile at the Penglaitan section of Laibin, Guangxi Province, and its geological implications [J]. *Acta Geological Sinica*, 2009, 83(1): 1–15.

- 云南省地质矿产局. 云南省区域地质志 [M]. 北京: 地质出版社, 1990.
- YUNNAN Bureau of Geology and Mineral Resources. Regional Geological Records of Yunnan Province [M]. Beijing: Geology Press, 1990.
- 钟大赉. 漾川西部古特提斯造山带 [M]. 北京: 科学出版社, 1998.
- ZHONG Dalai. The paleo Tethyan orogenic belt in western Yunnan and Sichuan [M]. Beijing: Science Press, 1998.
- Adachi M, Yamamoto K, Sugisaki R. Hydrothermal chert and associated siliceous rocks from the Northern Pacific: Their geological significance as indication of ocean ridge activity [J]. *Sedimentary Geology*, 1986, 47(1-2): 125–148.
- Bau M, Koschinsky A, Dulski P, et al. Comparison of the partitioning behaviours of yttrium, rare earth elements, and titanium between hydrogenetic marine ferromanganese crusts and seawater [J]. *Geochimica et Cosmochimica Acta*, 1996, 60(10): 1709–1725.
- Chakrabarti R, Knoll A H, Jacobsen S B, et al. Si isotope variability in Proterozoic cherts [J]. *Geochimica et Cosmochimica Acta*, 2012, 91: 187–201.
- Chen D Z, Qing H R, Yan X, et al. Hydrothermal venting and basin evolution (Devonian, South China): constraints from rare earth element geochemistry of the chert [J]. *Sedimentary Geology*, 2006, 183(3-4): 203–216.
- Chun Kit Lai, Sébastien Meffre, Anthony J C, et al. The central Ailaoshan ophiolite and modern analogs [J]. *Gondwana Research: International Geoscience Journal*, 2014, 26(1): 75–88.
- Elderfield H G, Greaves M J. The rare earth elements in seawater [J]. *Nature*, 1982, 296: 214–219.
- Fan H F, Wen H J, Zhu X K, et al. Hydrothermal activity during Ediacaran-Cambrian transition: Silicon isotopic evidence [J]. *Precambrian Research*, 2013, 224: 23–35.
- Fan W M, Wang Y J, Zhang F F, et al. Permian arc-back-arc basin development along the Ailaoshan tectoniczone: Ceochemical, isotopic and geochronol evidence from the Mojiang volcanic rocks, Southwest china [J]. *Lithos*, 2010, 119(3-4): 553–568.
- Fleet A J. Hydrothermal and hydrogenous ferro-manganese deposits: Do they from a continuum? The rare earth element evidence. In: Rona P A, Bostrom K, Laubier L, Smith K L, eds. *Hydrothermal Process at Seafloor Spreading Centers* [J]. New York: Plenum Press, 1983, 535–555.
- Girty G H, Ridge D L, Knaack C, et al. Provenance and depositional setting of Paleozoic chert and argillite, Sierra Nevada, California [J]. *Journal of Sedimentary Research*, 1996, 66(1): 107–118.
- Hara H, Kurihar T, Kurod J, et al. Geological and geochemical aspects of a Devonian siliceous succession in Northern Thailand: Implications for the opening of the Paleo-Tethys [J]. *Palaeogeography, Palaeoclimatology, Palaeoecology*, 2010, 297(2): 432–464.
- Huang Hu, Du Yuansheng, Huang Zhiqiang, et al. Depositional chemistry of chert during Late Paleozoic from western Guangxi and its implication for the tectonic evolution of the Youjiang Basin [J]. *Science China: Earth Sciences*, 2013, 43(2): 304–316.
- Jian P, Liu D Y, Kröner A, et al. Devonian to Permian platetectonic cycle of the Paleo-Tethys Orogen in southwest China (I): Geochemistry of ophiolites, arc/back-arc assemblages and within-plate igneous rocks [J]. *Lithos*, 2009a, 113: 748–766.
- Jian P, Liu D Y, Kröner A, et al. Devonian to Permian platetectonic cycle of the Paleo-Tethys Orogen in southwest China (II): Insights from zircon ages of ophiolites, arc/back-arc assemblages and within-plate igneous rocks and generation of the Emeishan CFB province [J]. *Lithos*, 2009b, 113: 767–784.
- Jones J H, Hart S R. Extreme Incompatibility of Pb during the Crystallization of Magmatic Iron-Meteorites [J]. *Meteoritics*, 1994, 19(4): 248–248.
- Lewis K H, Garwood R J, Brasier M D, et al. Carbonaceous microstructures from sedimentary laminated chert within the 3.46 Ga Apex Basalt, Chinaman Creek locality, Pilbara, Western Australia [J]. *Precambrian Research*, 2016, 278: 161–178.
- Metcalfe I. Palaeozoic and Mesozoic tectonic evolution and palaeogeography of East Asian crustal fragments: The Korean Peninsula in context [J]. *Gondwana Research*, 2006, 9: 24–46.
- Metcalfe I. Gondwana dispersion and Asian accretion: Tectonic and palaeogeographic evolution of eastern Tethys [J]. *Journal of Asian Earth Sciences*, 2013, 66: 1–33.
- Miroshnichenko N V, Perevoznikova Y V. The Intermetallic Compound Ni₃Au and Gold-Nickel Solid Solutins in Metalliferous Sediments of the Triassic Chert Formation in Sikhote-Alin in the Far East [J]. *Russian Journal of Pacific Geology*, 2010, 4(1): 56–62.
- Molnar P and Tapponnier P. Cenozoic tectonics of Asia: Effects of a continental collision [J]. *Science*, 189(4201): 1975, 419–426.
- Murray R W. Chemical criteria to identify the depositional environment of chert: general principles and application [J]. *Sedimentary Geology*, 1994, 90: 213–232.
- Murray R W, Buchholtz T, Brink M R, et al. Rare earth elements as indicators of different marine depositional environments in chert and shale [J]. *Geology*, 1990, 18: 268–271.
- Murray R W, Buchholtz T, Brink M R, et al. Rare earth, major, and trace elements in chert from Franciscan Complex and Monterey Group: Assessing REE sources to fine-grained marine sediments [J]. *Geochimica et Cosmochimica Acta*, 1991, 55(7): 1875–1895.

- Murray R W, Buchholtz Ten Brink M R, Gerlach D C, et al. Rare earth, major, and trace element composition of Monterey and DSDP chert and associated host sediment: Assessing the influence of chemical fractionation during diagenesis[J]. *Geochimica et Cosmochimica Acta*, 1992, 56(7): 2657–2671.
- Pan G T, Wang L Q, Li R S, et al. Tectonic evolution of the Qinghai-Tibet Plateau[J]. *Journal of Asian Earth Sciences*, 2012, 53: 3–14.
- Schärer U, Tapponnier P, Lacassin R, et al. Intraplate tectonics in Asia: A precise age for large-scale Miocene movement along the Ailao Shan – Red River shear zone[J]. *China Earth and Planetary Science Letters*, 1990, 97(1-2): 65–77.
- Tapponnier P, Lacassin R, Leloup P H, et al. The Ailaoshan/Red River metamorphic belt: Tertiary left-lateral shear between Indochina and South China[J]. *Nature*, 1990, 343(6257): 431–437.
- Taylor S R, McLennan S M. The Continental Crust, Its Composition and Evolution: an Examination of the Geochemical Record Preserved in Sedimentary Rocks [M]. Oxford: Blackwell Scientific Publications, 1985, 1–312.
- Thassanapak H, Uddachachon M, Chonglakmani C, et al. Geochemistry of Middle Triassic radiolarian cherts from northern Thailand: Implication for depositional environment[J]. *Journal of Earth Science*, 2011, 22(6): 688–703.
- Thurston P C, Kamber B S, Whitehouse M. Archean cherts in banded iron formation: insight into Neoarchean Ocean chemistry and depositional processes[J]. *Precambrian Research*, 2012, 214–215: 227–257.
- Wang Q F, Deng J, Li C S, et al. The boundary between the Simao and Yangtze blocks and their locations in Gondwana and Rodinia: Constraints from detrital and inherited zircons[J]. *Gondwana Research*, 2014, 26: 438–448.
- Xia X P, Nie X S, Lai C K, et al. Where was the Ailaoshan Ocean and when did it open: A perspective based on detrital zircon U-Pb age and Hf isotope evidence[J]. *Gondwana Research*, 2016, 36: 488–502.
- Xu J F, Castillo P R. Geochemical and Nd-Pb isotopic characteristics of the Tethyan asthenosphere: implications for the origin of the Indian Ocean mantle domain[J]. *Tectonophysics*, 2004, 393 (1–4): 9–27.
- Yin Leiming, Borjiginb Tenger, Knolle Andrew H, et al. Sheet-like microfossils from hydrothermally influenced basinal cherts of the lower Cambrian (Terreneuvian) Niutitang Formation, Guizhou, South China[J]. *Palword*, 2016, 350: 1–11.